

Lawrence Berkeley National Laboratory

Recent Work

Title

STOCHASTIC ACCELERATION BY AN OBLIQUELY PROPAGATING WAVE?AN EXAMPLE OF OVERLAPPING RESONANCES

Permalink

<https://escholarship.org/uc/item/0xr3b7c8>

Author

Smith, Gary R.

Publication Date

1978-04-01

Submitted to Physics of Fluids

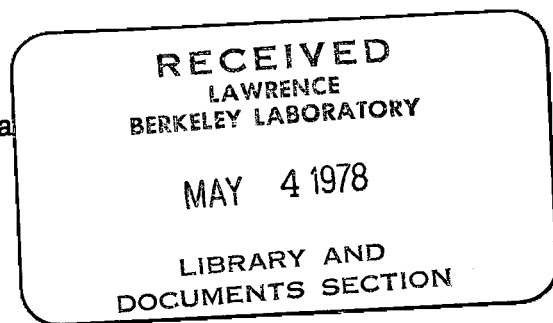
LBL-7555
Preprint

C.2

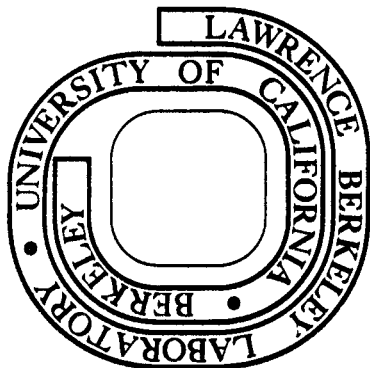
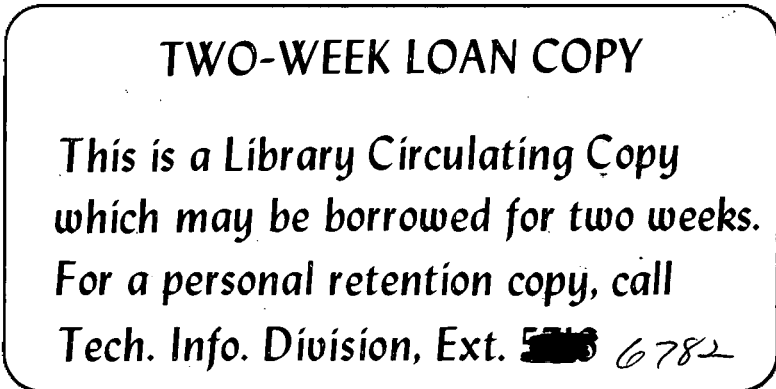
STOCHASTIC ACCELERATION BY AN OBLIQUELY
PROPAGATING WAVE--AN EXAMPLE OF
OVERLAPPING RESONANCES

Gary R. Smith and Allan N. Kaufman

April 10, 1978



Prepared for the U. S. Department of Energy
under Contract W-7405-ENG-48



LBL-7555

C.2

DISCLAIMER

This document was prepared as an account of work sponsored by the United States Government. While this document is believed to contain correct information, neither the United States Government nor any agency thereof, nor the Regents of the University of California, nor any of their employees, makes any warranty, express or implied, or assumes any legal responsibility for the accuracy, completeness, or usefulness of any information, apparatus, product, or process disclosed, or represents that its use would not infringe privately owned rights. Reference herein to any specific commercial product, process, or service by its trade name, trademark, manufacturer, or otherwise, does not necessarily constitute or imply its endorsement, recommendation, or favoring by the United States Government or any agency thereof, or the Regents of the University of California. The views and opinions of authors expressed herein do not necessarily state or reflect those of the United States Government or any agency thereof or the Regents of the University of California.

STOCHASTIC ACCELERATION BY AN OBLIQUELY PROPAGATING WAVE--
AN EXAMPLE OF OVERLAPPING RESONANCES

Gary R. Smith^{a)} and Allan N. Kaufman

Department of Physics and Lawrence Berkeley Laboratory,
University of California, Berkeley, CA 94720

ABSTRACT

We treat a simple problem exhibiting intrinsic stochasticity: the motion of a charged particle in a uniform magnetic field and a single plane wave. Our detailed studies of this wave-particle interaction show the following features. An electrostatic wave propagating obliquely to the magnetic field causes stochastic motion if the wave amplitude exceeds a certain threshold. The overlap of cyclotron resonances then destroys a constant of the motion, allowing appreciable momentum transfer to the particles. A wave of large enough amplitude would thus suffer severe damping and lead to rapid heating of a particle distribution. The stochastic motion resembles a diffusion process even though the wave spectrum is monochromatic. Our methods should be useful for other problems showing stochasticity. These problems include superadiabaticity in mirror machines, destruction of magnetic surfaces in toroidal systems, and lower hybrid heating.

I. INTRODUCTION

The interaction between a wave and a charged particle is of fundamental importance in plasma physics. In treating this interaction, one finds the concept of resonance to be useful. A problem involving a single resonance is the one-dimensional motion of an electron in a Langmuir wave, in which the resonance condition is $\omega = kv$. Such problems can be solved exactly,¹ allowing description of the bouncing motion of trapped particles, for example.

Generally, wave-particle interaction problems involve multiple resonances. Particle motion is qualitatively different depending on whether these resonances overlap (the concept of overlapping resonances is discussed in Sec. VII of this paper). Multiple resonances which do not overlap lead to no fundamental difficulties, but when two or more resonances overlap, the motion becomes incredibly complicated. Numerical solutions of the motion of such systems show a complexity which clearly cannot be described analytically; we cannot write, for example, an equation describing the evolution of a distribution of particles when two resonances overlap.

The term which has come into use to describe motion in the presence of overlapping resonances is "stochastic."² The stochasticity we study is intrinsic to the dynamical system:

the differential equations that determine the motion contain neither random coefficients nor random forces (nor are the initial conditions random). This intrinsic stochasticity arises from a fundamental mixing process: an arbitrarily small element of the phase-space fluid develops, exponentially in time, into a complicated filamentary structure, stretching throughout a large fraction of the accessible phase space. This mixing process, which accompanies the overlap of resonances, leads to irreversible macroscopic effects, like a coarse-grained entropy that increases in time.

In this paper we treat a simple problem involving overlapping cyclotron resonances. The resonance conditions are

$$\omega = k_z v_z - \ell \Omega, \quad (1)$$

where $\Omega \equiv eB_0/mc$ is the cyclotron (or gyro-) frequency of the particle of charge e and mass m , v_z is the particle's velocity parallel to a uniform, magnetostatic field $\mathbf{B} = B_0 \hat{z}$, ω and k_z are the frequency and parallel wavenumber of the wave, and ℓ is any integer. The resonances (1) are responsible for cyclotron-harmonic³ (or gyro-resonant) damping and growth of waves in a uniformly magnetized plasma.

Overlap of resonances can occur in many problems important

to the magnetic fusion energy program. In a nonuniform magnetic field ions can move stochastically in the presence of a wave driven to large amplitudes by an instability. Such problems have been studied for a tokamak^{4,5} and for a mirror machine.^{6,7} Stochastic ion motion may also be caused by a wave launched for radio-frequency heating of a tokamak plasma. This result was found for the lower-hybrid heating scheme by Karney and Bers⁸ and by Fukuyama, et al.⁹

For closed magnetic-confinement systems the question of the integrity of magnetic surfaces presents a number of important problems. Destruction of the surfaces (also known as magnetic braiding¹⁰ or stochasticity of field lines) can be caused by coil construction errors.¹¹⁻¹⁷ In the absence of coil construction errors destruction of magnetic surfaces can still occur because of current perturbations in the plasma. The current perturbations grow to large amplitudes because of unstable internal kink^{18,19} or tearing²⁰ modes. Finn^{21,22} and Stix²³ considered the hypothesis that the serious disruptive instability is caused by destruction of magnetic surfaces. Rechester and Stix²⁴ studied the destruction of the outer contours of magnetic islands. Recent theoretical work has suggested that instabilities in tokamaks might lead to overlapping micromagnetic islands.^{25,26} The overlapping islands would cause anomalous

transport of electron heat.²⁷

In reporting our work on overlapping cyclotron resonances we have two goals. First, we hope to stimulate interest in the experimental observation of our stochastic-acceleration process. Second, we believe our analytical and numerical methods are useful to workers studying overlapping resonances of any type.

Published accounts of our early work on the overlap of cyclotron resonances appear in Refs. 28 and 29.

The remainder of this paper is organized as follows. In Sec. II we give the considerations involved in choosing our model problem. Section III introduces the canonical variables we have found convenient. In Sec. IV we write the Hamiltonian and note some constants of the motion. In Sec. V we find some results which are valid when resonances do not overlap. In Sec. VI we find the behavior, in certain limits, of quantities which we later study numerically; the behavior is the same whether resonances overlap or not. In Sec. VII we apply a simple analytical criterion (overlap of resonances) for the onset of stochastic motion. To prepare for the description of our numerical results we briefly discuss the method of numerical integration (in Sec. VIII) and the surface of section method (Sec. IX). We present our numerical results in Sec. X. Section XI discusses some electrostatic waves which could cause appre-

ciable ion acceleration due to the overlap of cyclotron resonances. In Sec. XII we calculate the distortion of the tail of a Maxwellian distribution in the presence of such a wave. Appendix A explores the possibility of stochastic acceleration due to an electromagnetic wave. In Appendix B we mention the problem of motion in a nonsinusoidal wave. Appendix C gives requirements for observing stochastic acceleration in a laboratory experiment.

II. CHOICE OF MODEL

The motion of a particle in a uniform magnetic field and a sinusoidal plane wave exhibits a set of resonances which can overlap. From (1) we find the resonant parallel velocities

$$v_z = (\omega + l\Omega)/k_z ; \quad (2)$$

these velocities are finite if $k_z \neq 0$. The resonances have a non-zero width when the wave amplitude is not infinitesimal and the gyroradius is finite ($k_\perp \rho > 0$). Overlap of the resonances is thus possible if the wave propagates at an oblique angle to the magnetic field: $k_z, k_\perp \neq 0$.

Our work assumes the wave spectrum is so narrow that a single wave is a good representation of the spectrum. This situation is easiest to treat analytically and leads to the most

striking results.

We usually assume that the wave is electrostatic ($k_{\parallel} \parallel E_{\parallel}$). An electromagnetic wave can also cause stochastic acceleration since the same resonances occur as in the electrostatic case. The widths of the resonances are different and, as is shown in Appendix A, a wave amplitude large enough to cause overlap of the resonances is more difficult to achieve in the electromagnetic case.

Appendix B mentions the analytical complications which would arise if we relaxed our assumption that the wave is sinusoidal.

Finally, we assume that the amplitude Φ_0 of the electrostatic wave is constant in time. An antenna which launches a wave in a steady-state plasma will produce a constant wave amplitude. If, instead, the wave is due to an instability, then an equilibrium will be reached in which the linear growth rate γ_L balances the nonlinear damping rate $\gamma_S(\Phi_0)$ caused by stochastic acceleration of the particles. (We assume here that stochastic acceleration saturates the instability before any other nonlinear effect is important; this assumption must be investigated separately for each physical situation). We will find that stochastic acceleration is a very rapid process (characteristic rates comparable to the gyrofrequency Ω). Therefore, even

a variation in the wave amplitude at a quite rapid ($\sim 0.1 \Omega$) rate will not alter our results qualitatively.

III. CHOICE OF VARIABLES

To describe the motion of a particle, we could use the Cartesian variables (x, y, z, v_x, v_y, v_z) . Our work is simplified by choosing other variables and by using a Hamiltonian formulation. The simplest formulation is found by choosing generalized coordinates \underline{q} and momenta \underline{p} such that the motion in the magnetic field with no wave is described by a Hamiltonian depending on the momenta only: $H_0 = H_0(p)$.

We derive the uniform magnetic field $B_0 \hat{z}$ from the vector potential $\underline{A}_0(y) = -B_0 y \hat{x}$. The unperturbed (i.e., $\Phi_0 = 0$) Hamiltonian is

$$H_0(y, p_x, p_y, p_z) = \frac{1}{2} m v^2 = \frac{(\underline{p} + m\Omega y \hat{x})^2}{2m}.$$

We transform the perpendicular variables (x, y, p_x, p_y) to a new set of variables that describe the position of the guiding center and the gyration about it. We use the variables

$$\begin{aligned} \underline{q} &= (z, \phi, Y) \\ \underline{p} &= (p_z, p_\phi, m\Omega X), \end{aligned}$$

where ϕ is the gyrophase, p_ϕ the canonical angular momentum of gyration, and X and Y the components of the guiding center. These variables are defined in terms of the Cartesian variables by

$$\phi \equiv \tan^{-1} [(p_x + m\Omega y)/p_y]$$

$$p_\phi \equiv [(p_x + m\Omega y)^2 + p_y^2]/2m\Omega$$

$$Y \equiv -p_x/m\Omega$$

$$X \equiv x + p_y/m\Omega$$

The requirements for these variables to be canonical are easily verified by computing the Poisson brackets

$$[\phi, p_\phi] = (Y, m\Omega X) = 1$$

$$[\phi, Y] = [\phi, X] = [p_\phi, Y] = [p_\phi, X] = 0$$

The gyroradius ρ , the perpendicular velocity v_\perp , and the magnetic moment μ are defined in terms of p_ϕ by

$$p_\phi \equiv \frac{1}{2} m \Omega \rho^2 \equiv m v_\perp^2 / 2\Omega \equiv (mc/e)\mu$$

We write

$$\phi = \sin^{-1}(-v_x/v_{\perp}) = \cos^{-1}(-v_y/v_{\perp})$$

$$Y = y + \rho \sin \phi$$

$$X = x - \rho \cos \phi$$

to show that our names for ϕ , ρ , X , and Y correspond to their conventional meanings. However, we must warn the reader that when a time-varying electric field is present, as in this paper, our X and Y differ from the conventional guiding-center positions by the polarization shift, which equals the time integral of the polarization drift. We illustrate in Fig. 1 our definition of the gyrophase ϕ .

The unperturbed Hamiltonian is now written

$$H_0(p_z, p_{\phi}) = p_z^2/2m + p_{\phi}\Omega \quad (3)$$

In terms of the chosen variables the unperturbed motion is extremely simple:

$$\dot{H}_0 = \dot{p}_z = \dot{p}_{\phi} = \dot{X} = \dot{Y} = 0$$

$$\dot{z} = p_z/m = v_z$$

$$\dot{\phi} = \Omega .$$

(The dot denotes a total derivative with respect to time.)

IV. HAMILTONIAN

The total Hamiltonian is

$$H = H_0 + V \quad , \quad (4)$$

where H_0 is the unperturbed part (3) and V is the perturbation due to the wave. We use canonical variables that measure the position $z' = z - (\omega/k_z) t$ and parallel momentum $p_z' = p_z - m\omega/k_z$ in the wave frame. This reference frame moves at velocity $(\omega/k_z)\hat{z}$ with respect to the center of mass of the plasma. The canonical transformation to the wave-frame variables is a mathematical, not a physical (Galilean) transformation, and there is no requirement, as noted by Palmadesso,³⁰ that $\omega/k_z \ll c$. Nevertheless, we apply the transformation only to waves for which $\omega/k_z \ll c$, because these slow waves seem to lead to the strongest stochastic effects. For simplicity of notation we henceforth drop the primes on the wave-frame variables.

In the wave frame the perturbation due to the sinusoidal electrostatic wave is

$$V = e\phi_0 \sin(\mathbf{k}_{ww} \cdot \mathbf{x}_{ww}) \quad . \quad (5)$$

We choose the direction of the x-axis so that

$\underline{k} = k_z \hat{z} + k_\perp \hat{y}$, $k_\perp > 0$. Then, in terms of the variables discussed in Sec. III

$$V = e\phi_0 \sin(k_z z + k_\perp Y - k_\perp \rho \sin \phi) .$$

We redefine the origin of z by performing a canonical transformation to the new variables

$$z'' = z + k_\perp Y / k_z , \quad p_z'' = p_z$$
$$Y'' = Y, \quad X'' = X - k_\perp p_z / k_z m \Omega .$$

Since Y'' and X'' do not appear in the transformed Hamiltonian, they are each constants of the motion. Y'' is constant because there is no E_x to cause an $\underline{E} \times \underline{B}$ drift of the guiding center in the y -direction. X'' is constant because the electric field components E_y and E_z , which are related by $k_z E_y = k_\perp E_z$, cause, respectively, an $\underline{E} \times \underline{B}$ drift in the x -direction and an acceleration in the z -direction. The constancy of Y'' and X'' has been shown earlier³¹ using less powerful methods. We drop the primes on the new variables and write the perturbation in the final form

$$V(z, \phi, p_\phi) = e\Phi_0 \sin(k_z z - k_\perp \rho \sin \phi) \quad (6)$$

The Hamiltonian given by (3), (4), and (6) does not depend on time; therefore

$$\begin{aligned} H(z, \phi, p_z, p_\phi) &= p_z^2/2m + p_\phi \Omega + e\Phi_0 \sin(k_z z - k_\perp \rho \sin \phi) \quad (7) \\ &= E = \text{const}, \end{aligned}$$

the particle's energy in the wave frame is constant. In the plasma frame (7) becomes

$$\frac{1}{2} m [(v_z - \omega/k_z)^2 + v_\perp^2] + e\Phi_0 \sin(\mathbf{k} \cdot \mathbf{x} - \omega t) = \text{const}.$$

This result has been noted previously by several authors.^{30,32}

V. PARTICLE MOTION IN A SMALL-AMPLITUDE WAVE

We prepare for our discussion of stochastic acceleration, which requires a large wave amplitude, by studying here the case of a small-amplitude wave.

We use the Bessel-function identity

$$\exp(i a \sin \phi) = \sum_{\ell=-\infty}^{\infty} J_\ell(a) \exp(i\ell\phi) \quad (8)$$

to write the perturbation (6) as

$$V = e\phi_0 \sum_{\ell} J_{\ell}(k_{\perp}\rho) \sin(k_z z - \ell\phi) . \quad (9)$$

Most of the terms in this sum over ℓ vary rapidly in time and are not expected, on physical grounds, to have a significant effect on the particle motion. We identify the rapidly varying terms by substituting into (9) the expressions

$$z = v_{z0}t + z_0, \quad \phi = \Omega t + \phi_0, \quad \rho = \rho_0 , \quad (10)$$

derived from the unperturbed Hamiltonian H_0 . (In (10) the subscript zero denotes the value of a quantity at $t = 0$.) We find that (9) contains the oscillating functions $\sin[(k_z v_{z0} - \ell\Omega)t + k_z z_0 - \ell\phi_0]$. The particle is in exact resonance with the ℓ th component of the wave if

$$k_z v_{z0} = \ell\Omega . \quad (11)$$

This condition is the same as (1) but is expressed in terms of the parallel velocity in the wave frame instead of the plasma frame.

If v_{z0} is far from satisfying (11) for any ℓ , then all

the terms in (9) vary rapidly and the unperturbed motion, (10) together with $v_z = v_{z0}$, is a reasonable approximation to the exact motion.

If v_{z0} is close to satisfying (11) for a particular $l = L$ but far from satisfying it for all other l , then the motion is approximately that given by the truncated Hamiltonian

$$H_L = H_0 + e\phi_0 J_L[k_\perp \rho(p_\phi)] \sin(k_z z - L\phi) .$$

Two constants of the motion exist in this approximation. Since H_L is independent of time, one constant is H_L itself. The coordinates z and ϕ appear only in the combination $k_z z - L\phi$, so we can trivially derive the second constant by transforming to new variables using the generating function³³

$$F_2(z, \phi, p_\psi, I_L) = (k_z p_\psi + mL\Omega/k_z) z + (I_L - Lp_\psi)\phi .$$

In terms of the old variables, the new ones are

$$\begin{aligned} \psi &= \partial F_2 / \partial p_\psi = k_z z - L\phi, \quad \phi' = \partial F_2 / \partial I_L = \phi \\ p_\psi &= (p_z - mL\Omega/k_z) / k_z, \quad I_L = p_\phi + Lp_\psi \end{aligned} \quad (12)$$

The Hamiltonian is

$$H_L(\psi, p_\psi, I_L) = H_0(p_\psi, I_L) + e\Phi_0 J_L[k_\perp \rho(p_\psi, I_L)] \sin \psi,$$

which is independent of ϕ' , showing that I_L is a constant of the motion. Other constants, combinations of the two constants H_L and I_L , have been derived previously^{30,34} using other methods.

We now derive a measure of the width of the resonance L , i.e., how close v_{z0} must be to $L\Omega/k_z$ for the L th term in (9) to be slowly varying in time. We write the approximate Hamiltonian H_L as

$$H_L(\psi, p_\psi) = p_\psi^2 k_z^2 / 2m + e\Phi_0 J_L \sin \psi, \quad (13)$$

where we have suppressed the dependence on I_L and dropped constant terms. If the dependence of J_L on p_ψ is negligibly weak, then equation (13) is the Hamiltonian found in several other familiar problems, e.g., the one-dimensional motion of a particle in a Langmuir wave and the motion of a (nonlinear) pendulum. A separatrix divides the ψp_ψ -plane into regions in which the motion is qualitatively different. Inside the separatrix the particle is "trapped": ψ is confined to and oscillates within a finite interval ($< 2\pi$) during the motion. Outside the separatrix the particle is "untrapped": ψ increases

(or decreases) monotonically in time. On the separatrix the value of H_L is $e\phi_0 J_L$, and the maximum deviation of p_ψ from zero is

$$\Delta p_\psi = 2 |me\phi_0 J_L|^{1/2}/k_z .$$

Using (12), we derive $2\Delta v_z = 2\Delta p_z/m \equiv w_L$, which we refer to as the trapping width:

$$w_L = 4 |e\phi_0 J_L(k_\perp \rho)/m|^{1/2} . \quad (14)$$

Three trapping widths are indicated on Fig. 2, which was produced by the surface of section method described in Sec. IX. Near the stable equilibrium point ($\psi = \pm \frac{1}{2}\pi$, if $e\phi_0 J_L \leq 0$) the particle has a bounce frequency

$$\omega_L = k_z |e\phi_0 J_L(k_\perp \rho)/m|^{1/2} = \frac{1}{4} k_z w_L . \quad (15)$$

To derive (14) we have eliminated terms from the complete Hamiltonian by using our physical intuition that rapidly varying terms do not significantly affect the particle motion. This elimination can be done rigorously using any of several averaging methods, as discussed by Nayfeh.³⁵ Higher-order effects of the

rapidly varying terms can be computed using these methods.

VI. "DIFFUSION" AND CORRELATIONS IN A LINEAR THEORY

In Sec. X we present numerical calculations showing particle diffusion when resonances overlap. Here we define the diffusion coefficient that we study, and show that, for short times, apparent "diffusion" can occur regardless of whether resonances overlap. True diffusion, for long times, is possible only when overlapping resonances cause loss of memory of initial conditions. The results of this section allow us to properly interpret the numerical calculations to be presented later.

Diffusion, whether true or only apparent, occurs when a correlation function decays in time. We begin this section by studying the temporal behavior of the autocorrelation function of the parallel acceleration:

$$C(\tau, t') \equiv \langle \dot{v}_z(t' + \tau) \dot{v}_z(t') \rangle . \quad (16)$$

The brackets denote an average over the phases $k_z z_0$ and ϕ_0 ,

$$\langle A \rangle \equiv \int_0^{2\pi} \frac{d(k_z z_0)}{2\pi} \int_0^{2\pi} \frac{d\phi_0}{2\pi} A , \quad (17)$$

with the subscript zero indicating that the value of a variable

at $t = 0$ is used. This average mimics the situation often found in the laboratory: the initial phases are uniformly distributed over the physically distinct values.

To calculate (16) we use the unperturbed ($\Phi_0 = 0$) orbits (10). These are the orbits used in linear theory (e.g., to find the growth rate of an unstable wave of infinitesimal amplitude), and it is clearly impossible to describe nonlinear effects, like resonance overlap, using them. The parallel acceleration is found from (9):

$$\dot{v}_z = -\frac{1}{m} \frac{\partial V}{\partial z} = -\frac{k_z e \Phi_0}{m} \sum_{\ell} J_{\ell}(a) \cos(k_z z - \ell \phi), \quad (18)$$

where $a \equiv k_{\perp} \rho_0$. Inserting (10) into (18) and calculating (16), we find

$$C(\tau) = C(0) \sum_{\ell} J_{\ell}^2(a) \cos[(k_z v_{z0} - \ell \Omega)\tau] \quad (19a)$$

$$= C(0) \cos(k_z v_{z0} \tau) J_0(2a \sin \frac{1}{2} \Omega \tau); \quad (19b)$$

where $C(0) \equiv \frac{1}{2} (k_z e \Phi_0 / m)^2$. Note that (19) is independent of t' . Formula 8.531.3 of Ref. 36 has been used to rewrite (19a) in the form (19b).

Many of our numerical calculations use $a=5$, so we study the shape of (19) for short times in the limit $a \gg 1$. For

initial conditions such that $k_z v_{z0} \ll a\Omega = k_\perp v_{\perp 0}$, and for $\tau \lesssim \min(2\pi/\Omega, (k_z v_{z0})^{-1})$, (19b) simplifies to

$$C(\tau) \approx C(0) J_0(a\Omega\tau) . \quad (20)$$

From (20) we see that the correlation function falls to zero in the short time $\tau \approx 2.4/a\Omega \approx 0.5/\Omega$ and then oscillates with a period $\tau_1 \approx 2\pi/a\Omega \approx 1.3/\Omega$. We have made plots⁴ comparing the correlation function $C(\tau)$ found analytically from (19), and from the approximation (20), and $C(\tau, t' = 0)$ found from numerical integration (see Sec. VIII) of the equations of motion. The behavior predicted by the approximate expression (20) is indeed observed for sufficiently short times.

Using our knowledge of the correlation function, we next study the diffusion $\langle(\Delta v_z)^2\rangle$ in parallel velocity, where

$$\Delta v_z(t) \equiv v_z(t) - v_{z0} = \int_0^t dt' \dot{v}_z(t') \quad (21)$$

and the brackets are again defined by (17). From the definition (16) we have

$$\langle (\Delta v_z)^2 \rangle \equiv \int_0^t dt' \int_{-t'}^{t-t'} d\tau C(\tau, t') \quad (22a)$$

$$= 2 \int_0^t d\tau \int_0^{t-\tau} dt' C(\tau, t') \quad (22b)$$

$$= 2 \int_0^t d\tau (t - \tau) C(\tau) \quad (22c)$$

In (22b) we first used the symmetry property $C(\tau, t') = C(-\tau, t' + \tau)$ and then interchanged the order of the integrations.

To predict the time-dependence of $\langle (\Delta v_z)^2 \rangle$ for short t , we use (20). For very short times, $t \lesssim \tau_0 \equiv (a\Omega)^{-1}$, (20) is nearly constant and (22c) yields

$$\langle (\Delta v_z)^2 \rangle \approx C(0)t^2 \quad (23)$$

For $\tau_0 < t < 2\pi/\Omega$, the main contribution to (22c) comes from $0 < \tau < \tau_0$, since $C(\tau)$ is small and rapidly oscillating for larger τ . Thus

$$\langle (\Delta v_z)^2 \rangle \approx 2 C(0) \tau_0 t, \quad (24)$$

and the predicted "diffusion" coefficient is

$$D \equiv \langle (\Delta v_z)^2 \rangle / 2t \quad (25a)$$

$$\approx C(0)\tau_0 = (k_z e\phi_0/m)^2 / 2a\Omega \approx 0.1 (k_z e\phi_0/m)^2 / \Omega. \quad (25b)$$

Tetreault³⁷ reached the same conclusion that apparent "diffusion" can occur for short times even though motion is not stochastic. He pointed out the role in this "diffusion" of the nonresonant terms in (18). Each term causes constant acceleration of the particle, which would lead to the quadratic behavior seen in (23), but the number of nonresonant terms decreases as $1/t$, resulting in the linear behavior in (24).

VII. CHIRIKOV CRITERION FOR STOCHASTICITY

In Sec. V we treated particle motion in a wave of amplitude small enough that at most one term in the perturbation (9) was slowly varying in time. Two terms can be slowly varying if a particle lies within a trapping half-width of each of two adjacent resonances (11):

$$|v_z - \ell\Omega/k_z| < \frac{1}{2}w_\ell$$

for both $\ell = L$ and $L + 1$. The constants of the motion H_L and I_L , found when only the term $\ell = L$ was retained, are not expected to remain constant when two terms are slowly varying. Numerical integrations of the equations of motion verify (see

Sec. X) that, in large regions of phase space, no constant exists except the Hamiltonian if the wave amplitude is large. The particle is thus free to move almost anywhere on the energy (hyper)surface. This freedom can result in important physical consequences; in the presence of a single, obliquely propagating wave, particles can be accelerated to high velocities (i.e., a distribution can be heated to high temperatures).

The criterion that resonances overlap has been studied extensively by Chirikov³⁸ and found to predict the disappearance of constants of the motion (i.e., the onset of stochasticity) with accuracy sufficient for physical applications. The criterion is simply that the sum of the half-widths of adjacent resonances exceed the separation δ between them:

$$\frac{1}{2}(w_L + w_{L+1}) > \delta \quad (26)$$

The separation (in parallel velocity) follows from the resonance condition (11):

$$\delta = \Omega/k_z \quad (27)$$

The Chirikov criterion for stochastic particle motion in an oblique, electrostatic wave is thus

$$2|e\Phi_0/m|^{1/2} [|J_L(k_\perp \rho)|^{1/2} + |J_{L+1}(k_\perp \rho)|^{1/2}] > \Omega/k_z. \quad (28)$$

If the Bessel functions have comparable amplitudes, then (28) can be replaced by the simpler formula

$$16|e\Phi_0 J_L(k_\perp \rho)/m| > (\Omega/k_z)^2. \quad (29)$$

We interpret (29) as follows. Particles with parallel velocity (in the wave frame) such that $|k_z v_z / \Omega - L| < \frac{1}{2}$ will tend to move stochastically if (29) is satisfied but nonstochastically if it is not. We compare (28) to the findings of our numerical experiments in Sec. X.

VIII. NUMERICAL INTEGRATION OF THE EQUATIONS OF MOTION

To test various aspects of the theory of stochasticity as applied to particle motion in an oblique, electrostatic wave, we perform numerical integrations of the equations of motion. The equations are derived from Hamiltonian (7):

$$\begin{aligned} \dot{z} &= \partial H / \partial p_z, & \dot{\phi} &= \partial H / \partial p_\phi, \\ \dot{p}_z &= -\partial H / \partial z, & \dot{p}_\phi &= -\partial H / \partial \phi. \end{aligned} \quad (30)$$

We choose units such that $m = k_z = \Omega = 1$ and write (30) explicitly as

$$\dot{z} = p_z \quad (31a)$$

$$\dot{\phi} = 1 - \epsilon k_{\perp} \rho^{-1} \sin \phi \cos \chi \quad (31b)$$

$$\dot{p}_z = -\epsilon \cos \chi \quad (31c)$$

$$\dot{p}_{\phi} = \epsilon k_{\perp} \rho \cos \phi \cos \chi, \quad (31d)$$

where

$$\epsilon \equiv k_z^2 e\phi_0 / m\Omega^2, \quad (32)$$

$$\chi \equiv z - k_{\perp} \rho \sin \phi,$$

and $\rho = (2p_{\phi})^{1/2}$. We avoid taking a square root by replacing (31d) by

$$\dot{\rho} = \epsilon k_{\perp} \cos \phi \cos \chi. \quad (31e)$$

The four equations of motion (31a, b, c, e) are integrated on a CDC 7600 computer. The integration scheme (Gear-Hindmarsh) utilizes standard predictor-corrector methods. The order of the method and the size of the integration step are adjusted automatically to optimize the efficiency of the integration. The maximum order available is twelve. In our integrations, a typical order is eight and a typical integration step is $\Delta t \sim 0.05\Omega^{-1}$.

Several checks of the integration accuracy were made. Since the Hamiltonian is independent of the time, its numerical value should be nearly conserved during the integration. The percentage change in the value of the Hamiltonian was 0.0005% in a typical integration time of $50 \Omega^{-1}$. A different integration scheme was used in the early stages of this work. During the changeover from the old to the new scheme we checked that the particle trajectories found by the two schemes were very close to each other. Also, the equations of motion could be integrated forward and then backward in time to see if the initial conditions were recovered. For stochastic trajectories, the most difficult ones to integrate, we could integrate forward for a time $\sim 10\Omega^{-1}$ and still recover the initial conditions fairly well.

Further comments on integration of the equations of motion can be found in Ref. 4.

IX. SURFACE OF SECTION METHOD

A particle trajectory resulting from integration of (31) lies on a three-dimensional energy surface which is contained in the four-dimensional phase space. Attempting to represent a trajectory by a curve in a three-dimensional space would be needlessly difficult and confusing. To answer the important

physical question of whether motion is stochastic, we need trajectory information only at certain, well-separated instants of time. In this section we describe the technique, known as the surface of section method, for selecting these instants of time and for constructing a plot using the retained trajectory information; we also discuss the utility of the method.

Poincare's³⁹ surface of section method considers the intersection of a trajectory with a cross-section of the phase space. The chosen cross-section must be crossed repeatedly by the trajectory; a convenient choice in our work is defined by the gyrophase $\phi = \pi$. The intersection of the trajectory with $\phi = \pi$ yields a set of points in a three-dimensional space with axes z, p_z , and p_ϕ . We then ignore the p_ϕ -coordinates of the points and plot the points in the $z p_z$ -plane (i.e., we project them onto the plane).

As we integrate the equations of motion forward in time, successive points on the surface of section plot are generated roughly once each gyroperiod. The points are iterates of an area-preserving mapping of the $z p_z$ -plane onto itself. Calculating the iterates using the Hamiltonian equations of motion is computationally time-consuming, and past workers^{38,40-43} have often replaced a Hamiltonian system by a discrete mapping thought to mimic more or less closely the actual physical

systems of interest. These mappings display transitions from nonstochastic to stochastic behavior as a parameter is varied, just as Hamiltonian systems do. Generally we prefer to use the Hamiltonian equations of motion and thereby eliminate uncertainty about the relation between the given physical system and a chosen mapping.

By looking at a surface of section plot we can tell immediately whether a particular trajectory shows stochastic motion (nonexistence of a constant of the motion). By examining plots for several values of the stochasticity parameter (our ϵ) and for various initial conditions we can quickly gain a comprehensive understanding of the dynamical system being studied.

The utility of a surface of section plot arises from its method of construction. If a constant of the motion I exists for a particular orbit, that orbit will be confined to a two-dimensional surface, the intersection of the energy hypersurface with the hypersurface $I=\text{const}$. The intersection of this two-dimensional surface with the surface of section $\phi = \pi$ is a curve in $z p_z p_\phi$ -space, and projection onto the $z p_z$ -plane yields a curve on which the set of trajectory points must lie. If no constant I exists, an orbit will visit a three-dimensional region of the energy hypersurface. That region intersects $\phi = \pi$ in a two-dimensional surface, which, after projection

appears as an area of the $z p_z$ -plane. Thus, a constant of the motion exists if trajectory points lie on a curve, while a constant does not exist if the points fill an area. Note that the surface of section method does not tell us the analytic form of the constant, if one exists.

X. DISCUSSION OF NUMERICAL RESULTS

To validate the theoretical work, we integrate (31) numerically, presenting many of the results as surface of section plots.

We first illustrate, in Fig. 2, three of the resonances (11) for a wave amplitude ϕ_0 small enough that the resonances do not overlap. The positivity of the gyroradius limits the motion of a particle with a given energy to the region between the dashed lines.

Next, in Fig. 3, we plot trajectories when the wave amplitude is large enough for resonances to overlap. Points representing nonstochastic trajectories have been connected by smooth curves. This plot illustrates the "divided phase space" which occurs at intermediate values of the wave amplitude: regions in which a constant of the motion (in addition to the energy) exists are interspersed with regions in which it does not exist. The shapes of some of the smooth curves in Fig. 3 were

calculated by Taylor and Laing.⁴⁴ Other curves, representing resonances other than (11), appear in Fig. 3 but cannot be calculated by their simple theory. Near each of the three "primary" resonances (11) we see a set of five smooth curves; each set represents a single trajectory and is referred to as a chain of islands. Each chain shows the existence of a "secondary" or bounce resonance, which we have studied in detail in Ref. 4.

To demonstrate the possibility of heating a distribution of particles by applying a single, obliquely propagating wave, we use the plots in Fig. 4. The plots are constructed by the surface of section method, but in contrast to Figs. 2 and 3, the trajectory points are projected onto the $v_{\perp}v_z$ -plane instead of the $z p_z$ -plane. Fig. 4 shows the motion in velocity space (i.e., the acceleration) of a group of particles that is specified precisely in the figure caption; the group is chosen to represent particles with certain values of the perpendicular and parallel velocities at $t = 0$. We consider a wave of frequency $\omega = 3.6\Omega$ and choose a value $v_z = -\omega/k_z$ for the parallel velocity (as measured in the wave frame). The chosen particles thus have zero parallel velocity (as measured in the plasma frame) at $t = 0$.

Fig. 4 contrasts the particle acceleration in a wave of relatively small ($\epsilon = 0.25$) or large ($\epsilon = 0.75$) amplitude. In the small amplitude case no particles in the chosen group move stochastically, and the particle velocities remain near their initial values. In the large amplitude case all of the particles move stochastically, appearing to diffuse throughout much of the semicircular annulus bounded by the dashed curves. The dashed curves give the limits on the particle motion which follow from conservation of energy (as measured in the wave frame): the wave can change the kinetic energy of a particle by $2e\phi_0$ at most, giving curves at speeds $(v^2 \pm 4 e\phi_0/m)^{1/2}$, where v is the initial speed. The time-averaged value of a particle's kinetic energy, as measured in the plasma frame, increases substantially in the large amplitude case. The vertical axis at the far left of Fig. 4 helps us see the extent of the increase in parallel kinetic energy.

Our numerical results indicate a transition to stochastic motion at $\epsilon \approx 0.50$ when the propagation angle and initial particle velocity have the values used in Fig. 4. To compare this numerical result to the theoretical formula (28) we insert the values $J_{-3} = -0.17$ and $J_{-4} = 0.051$ for Bessel functions of argument $k_{\perp}\rho = 2.24$ and find the condition for stochastic motion to be

$$\epsilon > 0.61 .$$

The agreement is as good as can be expected considering the crudeness of both the numerical measurement and the theory.

In Fig. 4 the numbers 0, 1, 2, 5, 6, 7 show the positions of a particle (with a certain z_0) after the indicated number of gyroperiods. The process of diffusion over the semicircular annulus seems quite rapid, and we now investigate this process more carefully. We numerically calculate the trajectories of 50 to 200 particles which have unique initial values v_1 and v_z but initial values $k_z z$ and ϕ arranged in a regular array (see Fig. 5). In Fig. 6 we plot, for a subset of the trajectories, the parallel velocity v_z vs. time. We first note the diffusion of v_z away from its initial value; in the next paragraph we study this diffusion quantitatively. Interesting features of some trajectories in Fig. 6 are periods of rapid change in v_z (large parallel acceleration) separated by periods of relatively constant v_z . These features can be understood by noting that, under some circumstances, the Hamiltonian system (7) resembles a discrete mapping (see Ref. 4 for details).

To study the diffusion process quantitatively, we use the numerically calculated trajectories to compute $\langle (\Delta v_z)^2 \rangle$, a quantity introduced in Sec. VI. The time variation of this

quantity typically has the form shown in Fig. 7. Quadratic and then linear dependences on time, as predicted by (23) and (24), are observed during the first gyroperiod or so. Thereafter, a deviation from the linear behavior, indicating either a larger or a smaller diffusion rate, generally occurs. An interpretation of this deviation which is consistent with our numerical results is the following. The rate of diffusion of a group of particles is primarily determined by their present velocities rather than by the past history of the group (i.e., a Markovian assumption has some validity). As a group of particles diffuses, some particles reach velocities for which the diffusion rate is, say, larger than it was at the initial velocity. The diffusion rate of the whole group then appears to increase. This interpretation is indicated on Fig. 7. For long times the diffusion process ceases because the group has spread out to fill the entire stochastic region of velocity space (see Fig. 4).

Only limited studies of the correlation function (16) were carried out because of difficulties described in Ref. 4.

XI. OBLIQUE, ELECTROSTATIC WAVES FOR ACCELERATION OF IONS

In Sec. X we used, as an example, an electrostatic wave with frequency $\omega = 3.6\Omega$, propagation angle $\theta = 45^\circ$, and various amplitudes measured by $\epsilon \equiv k_z^2 e\Phi_0/m\Omega^2$. We identify

here a particular wave with these properties and show that the amplitudes used are not unreasonably large.

We concentrate on waves appropriate for heating ions, but we note that often there exists, for each ion wave, an electron wave with analogous parameters which is appropriate for heating electrons. In Appendix C we collect the experimental requirements necessary for observing heating of either ions or electrons.

A plasma in a uniform magnetic field can support an obliquely propagating, electrostatic wave which we call an ion-acoustic wave. This wave is indicated in Fig. 8. The name "intermediate-frequency acoustic wave" is used in the old, but still useful, review by Stringer.⁴⁵ As long as θ is not too close to 90° , the frequency ω is given approximately by the unmagnetized formula

$$\omega \approx kc_s,$$

where $k^2 \equiv k_z^2 + k_\perp^2$, and the sound speed is given by $c_s^2 \equiv (T_e + 3T_i)/m_i$. Given the wave parameters $\omega = 3.6\Omega_i$ and $\theta = 45^\circ$ and the temperature ratio T_e/T_i , we calculate the damping rate of the wave using the formula (4.68) in Ichimaru⁴⁶ appropriate for Maxwellian distributions of electrons and ions. Just as in an unmagnetized plasma, we find a

weakening of the damping as T_e/T_i increases. The damping reaches a fairly small value when T_e/T_i is increased to 16: $\gamma \approx -0.04\omega$. Such a large temperature ratio would not be required in an unmagnetized plasma to reach this damping rate. With the temperature ratio 16 chosen we can calculate the ion thermal speed, $v_{Ti} \equiv (T_i/m_i)^{1/2}$, to be

$$v_{Ti} \approx 0.58\Omega_i/k_z \quad (33)$$

This speed is indicated on Fig. 4 by the hatched semicircle. The group of ions studied in Fig. 4 would thus have an initial perpendicular velocity 3.8 times the thermal speed.

We now express the wave amplitude given by $\epsilon = 0.5$ in more familiar terms. From the fluid equations describing an ion-acoustic wave, one easily derives a relation between the potential amplitude ϕ_0 and density amplitude $\delta n/n$:

$$\frac{\delta n}{n} = \frac{e\phi_0}{m_i c_s^2} \quad (34)$$

Using the standard formulas for the dielectric function D and the Debye length λ_D , we also find the expression

$$W \equiv \frac{1}{8\pi} \omega \frac{\partial D}{\partial \omega} \langle E^2 \rangle = \frac{\phi_0^2}{8\pi\lambda_D^2} = \frac{1}{2} n (e\phi_0)^2 / T_e \quad (35)$$

for the wave energy density W . Use of (33) and $T_e/T_i = 16$ allows us to write $\epsilon = 0.5$ as

$$e\phi_0 \approx \frac{3}{2} T_i \approx \frac{1}{11} T_e . \quad (36)$$

Substitution of (36) into (34) and (35) yields

$$\delta n/n \approx 1/13, \quad W \approx nT_i/15 . \quad (37)$$

The moderate numerical values in (37) appear to justify our use of the linear dispersion relation for the wave. Also, (37) gives the important result that stochasticity can occur at smaller amplitudes than nonlinear effects requiring $\delta n/n \sim 1$. For other wave parameters, however, stochasticity might not occur for any physically reasonable wave amplitude.

The low-frequency ion-acoustic wave

$$\omega \approx k_z c_s < \Omega_i ,$$

which is shown in Fig. 8, might also be used to heat ions. A large temperature ratio is again required to reduce the linear damping rate. This wave seems to lead to less dramatic heating of an ion distribution than the ion-acoustic wave with $\omega > \Omega_i$.

The difference between parallel velocities in the plasma frame and in the wave frame decreases as ω decreases (see Fig. 4). For small ω the constant energy curves in the two frames are close together, implying less possibility of dramatic changes in the distribution of parallel kinetic energy (as measured in the plasma frame).

We have considered other waves of a plasma in a uniform magnetic field but have found no wave with more favorable parameters than those given here. Lacking a definite optimization criterion, we have not performed a systematic variation of ω and θ . Values of θ close to 90° are of particular interest since many waves propagate nearly perpendicular to the magnetic field; the lower hybrid wave, important in rf heating studies for tokamaks, is one example. For parameters typical of lower-hybrid-heating experiments the condition (29) for overlap of cyclotron resonances cannot be satisfied. Ion motion may be stochastic, nevertheless, because of the overlap of other resonances, as shown in Refs. 8 and 9.

XII. HEATING OF A DISTRIBUTION FUNCTION

In Sec. X we showed that a group of particles with given parallel and perpendicular velocities at $t = 0$ may be heated by a single, oblique wave. Here we consider a Maxwellian

distribution of velocities at $t = 0$ and find the distortion of that distribution caused by the wave.

We use the following qualitative picture suggested by Fig. 4. An ion whose velocity satisfies (29) moves stochastically, ranging over that portion of the constant-energy semicircle defined by (29). An ion whose velocity does not satisfy (29) remains nearly fixed in velocity space. In the presence of a single, oblique wave of large amplitude the steady-state ion distribution must therefore be constant along the stochastic portions of the constant-energy semicircles and nearly Maxwellian in the nonstochastic regions of velocity space.

This picture is implemented by a computer program which modifies an initially Maxwellian distribution to obtain the steady-state distribution. The modification is accomplished by successively considering semicircular annuli in $v_{\perp} v_z$ -space, each of which represents particles with a small range of speeds. For each annulus the Maxwellian is integrated over the stochastic portion of the annulus to find the total number of stochastic ions in the annulus. This number is then redistributed over the stochastic portion of the annulus with a weighting proportional to the perpendicular velocity v_{\perp} . This weighting results in a distribution that is uniform over the three-dimensional $(v_x v_y v_z)$ kinetic energy surface.

The steady-state distribution in $v_{\perp} v_z$ -space is integrated over v_z to obtain the perpendicular distribution and over v_{\perp} to obtain the parallel distribution. In Fig. 9 we plot these distributions on a logarithmic scale. The horizontal (velocity) axes use a quadratic scale so that a Maxwellian appears as a straight line. The same wave frequency and propagation angle and the same ion thermal speed are used as for the ion-acoustic wave of Sec. XI.

The wave is seen to distort only the tails of the perpendicular and parallel distributions, not the bodies. The perpendicular distribution is distorted for $v_{\perp} \gtrsim 3v_{Ti}$ in the case $\epsilon = 0.75$. The distortion of the parallel distribution is highly asymmetric because ions tend to be accelerated to the parallel velocity of the wave frame, which is positive and much larger than the thermal speed. Although the distortions shown in Fig. 9 involve only a tiny fraction of the total number of ions, the changes in the populations of tail ions are quite dramatic.

The tiny fraction of ions which is stochastically accelerated by the wave can gain a substantial amount of energy as a result of the large velocity changes produced during stochastic acceleration. As a numerical example we consider the smaller amplitude case $\epsilon = 0.25$ for which 0.03% of the ions move stochastically. These ions increase their kinetic energy

by an amount roughly equal to half of the energy in the wave. We thus expect the propagation characteristics of the wave to be altered significantly when stochastic acceleration occurs.

XIII. CONCLUSIONS

We have studied the motion of a charged particle in a single (monochromatic) wave that is propagating obliquely to a uniform magnetic field. As the wave amplitude is increased, a constant of the motion disappears, allowing the motion to become stochastic. The Chirikov criterion of overlapping resonances gives a prediction for the onset of stochasticity in good agreement with the results of numerical integration of the equations of motion.

The resemblance of stochastic motion to a diffusion process has been observed numerically. The "diffusion" which occurs even in linear theory has been distinguished from the true diffusion caused by overlap of resonances.

We have considered the possibility of using the overlap of cyclotron resonances as a mechanism for heating a particle distribution. Choice of an electrostatic wave, the ion-acoustic wave, allows parameters satisfying the requirements of our analysis. The analysis predicts rapid transfer of wave energy to ions in the tails of the perpendicular and parallel distributions. Heating of ions by this mechanism does not appear impor-

tant in fusion plasmas but might be used in a small-scale laboratory experiment to observe stochastic acceleration by a single wave.

ACKNOWLEDGMENTS

We gratefully acknowledge extensive discussions of this work with John Krommes.

Work performed under the auspices of the U.S. Department of Energy by the Lawrence Berkeley Laboratory under contract number W-7405-Eng-48.

APPENDIX A: STOCHASTIC ACCELERATION BY AN ELECTROMAGNETIC WAVE

Stochastic acceleration by an electrostatic wave is treated in detail in this paper. Here we discuss the possibility that an electromagnetic wave could cause stochastic acceleration.

A charged particle in a uniform magnetic field plus a small-amplitude electromagnetic wave can be trapped near the resonances (1),³⁰ in complete analogy with the electrostatic case treated in Sec. V. Palmadesso³⁰ gives the constant of the motion analogous to (13); from his formulas we can deduce the trapping width in an electromagnetic wave of arbitrary polarization and propagation direction.

As an example of a particular electromagnetic wave we consider a high-frequency Alfvén wave propagating in the yz-plane. By this name we refer to a wave on the same branch as the magnetosonic (compressional Alfvén) and whistler waves but with a frequency a few times the ion gyrofrequency. The dispersion diagram in Fig. 8 shows the location of the high-frequency Alfvén wave. When the propagation angle $\theta = 0^\circ$ (i.e., $k_\perp = 0$), this wave is right-hand-circularly-polarized, and the trapping width is

$$w_\ell = 4 \left| e v_\perp B_x J_{\ell-1}(k_\perp \rho) / m_i c k_z \right|^{1/2}, \quad (A1)$$

where B_x is the amplitude of the x-component of the wave's magnetic field. When the wave propagation is oblique (k_z , $k_{\perp} \neq 0$), (A1) is still a good approximation for certain combinations of wave frequency ω and angle θ . When (A1) is valid, the condition of overlapping cyclotron resonances appears difficult to satisfy. Using the same values of $k_{\perp} \rho$ and $k_z v_z / \Omega$ (which determines ℓ) as in Fig. 4, we find the Bessel function $J_{\ell-1}$ to be smaller than J_{ℓ} by a factor of about three. A high-frequency Alfvén wave with amplitude given by

$$|k_z v_{\perp} e B_x / m_i c \Omega_i^2| = 1.5 \quad (A2)$$

could thus be expected to cause ion heating similar to that caused by the ion-acoustic wave of Sec. XI which has

$$k_z^2 e \Phi_0 / m_i \Omega_i^2 = 0.5 .$$

To check whether (A2) is a reasonable wave amplitude we calculate the fractional change in B_z due to the wave:

$$|\delta B_z / B_0| = |k_{\perp} B_x / k_z B_0| = 1.5 k_{\perp} / k_z^2 \rho \quad (A3)$$

For the linear cyclotron-harmonic damping of the wave to be weak we use the crude condition that the ion thermal speed satisfy

$$v_{Ti} \lesssim 0.5 \Omega_i / k_z \quad ; \quad (A4)$$

this condition means the distribution function "fits" between the resonant parallel velocities Ω_i / k_z (compare (33)). Combining (A3) and (A4) and taking $k_z = k_{\perp}$, we find that ions with $v_{\perp} \approx 4v_{Ti}$ are stochastically accelerated if

$$|\delta B_z / B_0| \gtrsim 0.75 \quad . \quad (A5)$$

A high-frequency Alfvén wave with amplitude (A5) would not obey the requirements of our analysis that the wave be sinusoidal and satisfy the linear relations for the frequency and polarization. On the basis of this example we conclude that an electromagnetic wave of reasonable amplitude is less likely to cause stochastic acceleration by overlap of cyclotron resonances than is an electrostatic wave. It is clear, however, that many choices of parameters were made in arriving at (A5), and the possibility of strong stochastic effects due to an electromagnetic wave cannot be ruled out.

APPENDIX B: STOCHASTIC ACCELERATION BY A NONSINUSOIDAL WAVE

The problem treated in detail in this paper involves stochastic motion caused by a sinusoidal wave. We note here that such motion can occur as well for a nonsinusoidal wave. Stochasticity might appear at a lower value of the wave amplitude in the nonsinusoidal case.

We consider a plane electrostatic wave for which the potential is an arbitrary periodic function of the phase $\underline{k} \cdot \underline{x} - \omega t$. As in Sec. IV we eliminate the time dependence by using wave-frame variables and write the perturbation as

$$V = e \sum_n \Phi_n \sin(n \underline{k} \cdot \underline{x} + \delta_n) ,$$

which replaces (5). The operations performed in Sec. IV allow us to write the equation

$$V(z, \phi, \rho_\phi) = e \sum_n \Phi_n \sin(nk_z z - nk_\perp \rho \sin\phi + \delta_n) ,$$

which replaces (6). Use of (8) now yields

$$V = e \sum_n \Phi_n \sum_\ell J_\ell(nk_\perp \rho) \sin(nk_z z - \ell\phi + \delta_n) . \quad (B1)$$

Analysis of (B1) by the method of Sec. V shows the existence of resonant velocities

$$v_z = (\ell/n)\Omega/k_z ,$$

which are distributed along the real number line as the rational numbers are distributed. The complications implied by this distribution have deterred us from study of nonsinusoidal waves. One might expect, however, that a nonsinusoidal wave would lead more easily to stochastic motion than a sinusoidal one because of the presence of the large number of additional resonances of finite width (proportional to $\phi_n^{1/2}$).

APPENDIX C: EXPERIMENTAL REQUIREMENTS FOR OBSERVING STOCHASTIC ACCELERATION

Stochastic acceleration of ions by a single ion-acoustic wave was seen in Secs. XI and XII to lead to the heating of a Maxwellian distribution. We believe a fairly simple laboratory experiment could observe these effects. When stochasticity occurs one should see a change in propagation characteristics of a launched, obliquely propagating wave, and one might observe a high-energy tail in the parallel distribution. Some care must be taken experimentally in launching an ion-acoustic wave in order to avoid effects mentioned in Refs. 47 and 48. Assuming that the desired wave can be launched, we give here the experimental requirements suggested by our theoretical work.

To observe ion tail-heating by an ion-acoustic wave, the following requirements must be met.

1. The wave frequency $\omega (\approx kc_s)$ should be a few times the ion gyrofrequency Ω_i , but not too close to a multiple of Ω_i to avoid cyclotron-harmonic damping.
2. The propagation angle θ with respect to the magnetostatic field \underline{B}_w should be in the vicinity of 45° .
3. The temperature ratio T_e/T_i should be high enough that the wave damping is small, but there must be

ions with gyroradii comparable to the perpendicular wavelength ($k_{\perp} \rho_i \gtrsim 1$).

4. The ion collision frequency ν_i must be less than about $0.1\Omega_i$ so the collisionless theory is applicable.
5. The wave amplitude should be uniform in the $\underline{k} \times \underline{B}$ direction over a distance L_x satisfying $k_z L_x \gtrsim \omega/\Omega_i$. Otherwise, ions $\underline{E} \times \underline{B}$ drift out of the wave before significant acceleration occurs.
6. The density amplitude must be as large as $\delta n/n \sim 0.1$.

To observe electron tail-heating by a Langmuir wave, the analogous requirements are the following.

1. $\omega(\approx \omega_{pe})$ a few times Ω_e , but not too close to a multiple of Ω_e .
2. $\theta \sim 45^\circ$.
3. The Debye length λ_D should be small enough ($k\lambda_D \lesssim 0.25$) that the wave damping is weak, but electrons with gyroradii such that $k_{\perp} \rho_e \gtrsim 1$ must exist.
4. $\nu_e \lesssim 0.1 \Omega_e$.
5. $k_z L_x \gtrsim \omega/\Omega_e$.
6. $\delta n_e/n_e \sim 0.1$.

REFERENCES

- a) Present address: Lawrence Livermore Laboratory, University of California, Livermore, CA 94550.
- ¹T. M. O'Neil, Phys. Fluids 8, 2255 (1965).
 - ²G. M. Zaslavskii and B. V. Chirikov, Usp. Fiz. Nauk 105, 3 (1971) [Sov. Phys.-Usp. 14, 549 (1972)].
 - ³J. A. Tataronis and F. W. Crawford, J. Plasma Phys. 4, 231 and 249 (1970).
 - ⁴G. R. Smith, Ph.D. thesis, University of California, Berkeley, 1977.
 - ⁵G. R. Smith, Phys. Rev. Lett. 38, 970 (1977).
 - ⁶M. N. Rosenbluth, Phys. Rev. Lett. 29, 408 (1972).
 - ⁷A. V. Timofeev, Nucl. Fusion 14, 165 (1974).
 - ⁸C. F. F. Karney and A. Bers, Phys. Rev. Lett. 39, 550 (1977).
 - ⁹A. Fukuyama, H. Momota, R. Itatani, and T. Takizuka, Phys. Rev. Lett. 38, 701 (1977).
 - ¹⁰T. H. Stix, Phys. Rev. Lett. 30, 833 (1973).

- ¹¹V. F. Aleksin, V. N. Pyatov, V. P. Sebko, and V. I. Tyupa, Zh. Tekh. Fiz. 45, 536 (1975) [Sov. Phys.-Tech. Phys. 20, 335 (1975)] and Fiz. Plazmy 2, 219 (1976) [Sov. J. Plasma Phys. 2, 120 (1976)].
- ¹²M. N. Rosenbluth, R. Z. Sagdeev, J. B. Taylor, and G. M. Zaslavskii, Nucl. Fusion 6, 297 (1966).
- ¹³N. N. Filonenko, R. Z. Sagdeev, and G. M. Zaslavskii, Nucl. Fusion 7, 253 (1967).
- ¹⁴B. S. Akshanov, N. A. Manzyuk, V. I. Muratov, V. N. Pyatov, V. P. Sebko, and V. I. Tyupa, Zh. Eksp. Teor. Fiz. Pis'ma Red. 21, 212 (1975) [JETP Lett. 21, 94 (1975)].
- ¹⁵R. P. Freis, C. W. Hartman, F. M. Hamzeh, and A. J. Lichtenberg, Nucl. Fusion 13, 533 (1973).
- ¹⁶F. M. Hamzeh, Nucl. Fusion 14, 523 (1974).
- ¹⁷S. L. Davis, R. J. Hawryluk, and J. A. Schmidt, Phys. Fluids 19, 1805 (1976).
- ¹⁸M. N. Rosenbluth, R. Y. Dagazian, and P. H. Rutherford, Phys. Fluids 16, 1894 (1973).
- ¹⁹B. Coppi, R. Galvão, R. Pellat, M. Rosenbluth, and P. H.

Rutherford, MATT-1271 (July 1976).

- ²⁰J. F. Drake and Y. C. Lee, Phys. Fluids 20, 1341 (1977).
- ²¹J. M. Finn, Nucl. Fusion 15, 845 (1975).
- ²²J. M. Finn, Phys. Fluids 20, 1749 (1977).
- ²³T. H. Stix, Phys. Rev. Lett. 36, 521 (1976).
- ²⁴A. B. Rechester and T. H. Stix, Phys. Rev. Lett. 36,
587 (1976).
- ²⁵L. Chen, P. H. Rutherford, and W. M. Tang, Phys. Rev. Lett.
39, 460 (1977).
- ²⁶J. Hsu, P. Kaw, and L. Chen, PPPL-1358, July 1977.
- ²⁷A. B. Rechester and M. N. Rosenbluth, Phys. Rev. Lett. 40,
38 (1978).
- ²⁸G. R. Smith and A. N. Kaufman, Phys. Rev. Lett. 34, 1613
(1975).
- ²⁹G. R. Smith and A. N. Kaufman, in Plasma Physics, ed. H.
Wilhelmsson (Plenum, New York, 1977), p. 475.
- ³⁰P. J. Palmadesso, Phys. Fluids 15, 2006 (1972).

- ³¹M. L. Woolley, Plasma Phys. 13, 1141 (1971).
- ³²T. H. Stix, Nucl. Fusion 15, 737 (1975).
- ³³H. Goldstein, Classical Mechanics (Addison-Wesley, Reading, Mass., 1965), Chap. 8.
- ³⁴A. B. Kitsenko, I. M. Pankratov, and K. N. Stepanov, Zh. Eksp. Teor. Fiz. 66, 166 (1974) [Sov. Phys.-JETP 39, 77 (1974)].
- ³⁵A. H. Nayfeh, Perturbation Methods (Wiley, New York, 1973).
- ³⁶I. S. Gradshteyn and I. M. Ryzhik, Tables of Integrals, Series, and Products (Academic, New York, 1965).
- ³⁷D. J. Tetreault, Ph.D. thesis, Massachusetts Institute of Technology, 1976.
- ³⁸B. V. Chirikov, Research Concerning the Theory of Non-linear Resonance and Stochasticity, (CERN Trans. 71-40, Geneva, 1971).
- ³⁹H. Poincaré, New Methods of Celestial Mechanics (Washington, National Aeronautics and Space Administration, 1967), vol. 3, p. 176.

- ⁴⁰M. Hénon and C. Heiles, *Astron. J.* 69, 73 (1964).
- ⁴¹C. Froeschlé, *Astron. and Astrophys.* 9, 15 (1970).
- ⁴²J. M. Greene, *J. Math. Phys.* 9, 760 (1968).
- ⁴³M. A. Lieberman and A. J. Lichtenberg, *Phys. Rev. A* 5, 1852 (1972).
- ⁴⁴J. B. Taylor and E. W. Laing, *Phys. Rev. Lett.* 35, 1306 (1975).
- ⁴⁵T. E. Stringer, *Plasma Phys.* 5, 89 (1963).
- ⁴⁶S. Ichimaru, Basic Principles of Plasma Physics (Benjamin, Reading, Mass., 1973).
- ⁴⁷T. Christensen and N. Hershkowitz, *Phys. Fluids* 20, 840 (1977).
- ⁴⁸T. Chen and L. Schott, *Phys. Fluids* 20, 844 (1977).

FIGURE CAPTIONS

FIG. 1. Specification of the particle position (x, y) in terms of the canonical variables used in the text.

FIG. 2. Surface of section plot illustrating three non-overlapping resonances. The initial conditions, indicated by X's, were chosen to yield trajectories very close to the three separatrices. The points representing the trajectories have been connected with hand-drawn curves. The wave amplitude is given by $\epsilon = 0.025$, the other parameters are $k_{\perp} \rho_E \equiv k_{\perp} (2E/m)^{1/2} / \Omega = 1.48$, and $\theta \equiv \tan^{-1}(k_{\perp}/k_z) = 45^\circ$.

FIG. 3. Surface of section plot showing a divided phase space. The parameters are the same as in Fig. 2, except $\epsilon = 0.1$.

FIG. 4. Surface of section plots contrasting the motion in velocity space in the presence of a small- or of a large-amplitude wave. The wave has frequency $\omega = 3.6\Omega$ and propagation angle $\theta = 45^\circ$. Trajectories of a group of ten particles are represented. At $t = 0$ this group has values of $k_z z = N\pi/5$, $N = 0, 1, 2, \dots, 9$, but has unique values of $\phi (= \pi)$, v_{\perp} , and v_z . The chosen value of the perpendicular velocity is given by $k_z v_{\perp} / \Omega = k_{\perp} \rho = 2.24$ and of the parallel velocity by $k_z v_z / \Omega = -3.6$. The hatched semicircle shows the

extent of the thermal ions considered in the wave-heating example of Secs. XI and XII.

FIG. 5. Array of 100 initial values of $k_z z$ and ϕ used to approximate numerically the average defined by (17).

FIG. 6. Particle trajectories, represented by plotting the parallel velocity vs. time. The wave amplitude is given by $\epsilon = 0.75$ and the propagation angle by $\theta = 45^\circ$. The initial speed ($v = 5\Omega/k_z$) and parallel velocity ($v_z = 0$) are the same for all trajectories, but the initial phases $k_z z$ and ϕ differ.

FIG. 7. The mean square deviation in parallel velocity vs. time. Parameters are the same as in Fig. 6.

FIG. 8. Dispersion diagram (ω vs. k) for a plasma in a uniform magnetic field, showing the high-frequency Alfvén wave (Appendix A), the ion-acoustic wave (Secs. XI and XII), and the low-frequency ion-acoustic wave (Sec. XI). Adapted from a figure in Ref. 45.

FIG. 9. The perpendicular (f_\perp) and parallel (f_\parallel) distribution functions in the presence of a finite-amplitude, obliquely propagating, electrostatic wave. The distortions to Maxwellian distributions ($\epsilon = 0$) are shown for two wave

extent of the thermal ions considered in the wave-heating example of Secs. XI and XII.

FIG. 5. Array of 100 initial values of $k_z z$ and ϕ used to approximate numerically the average defined by (17).

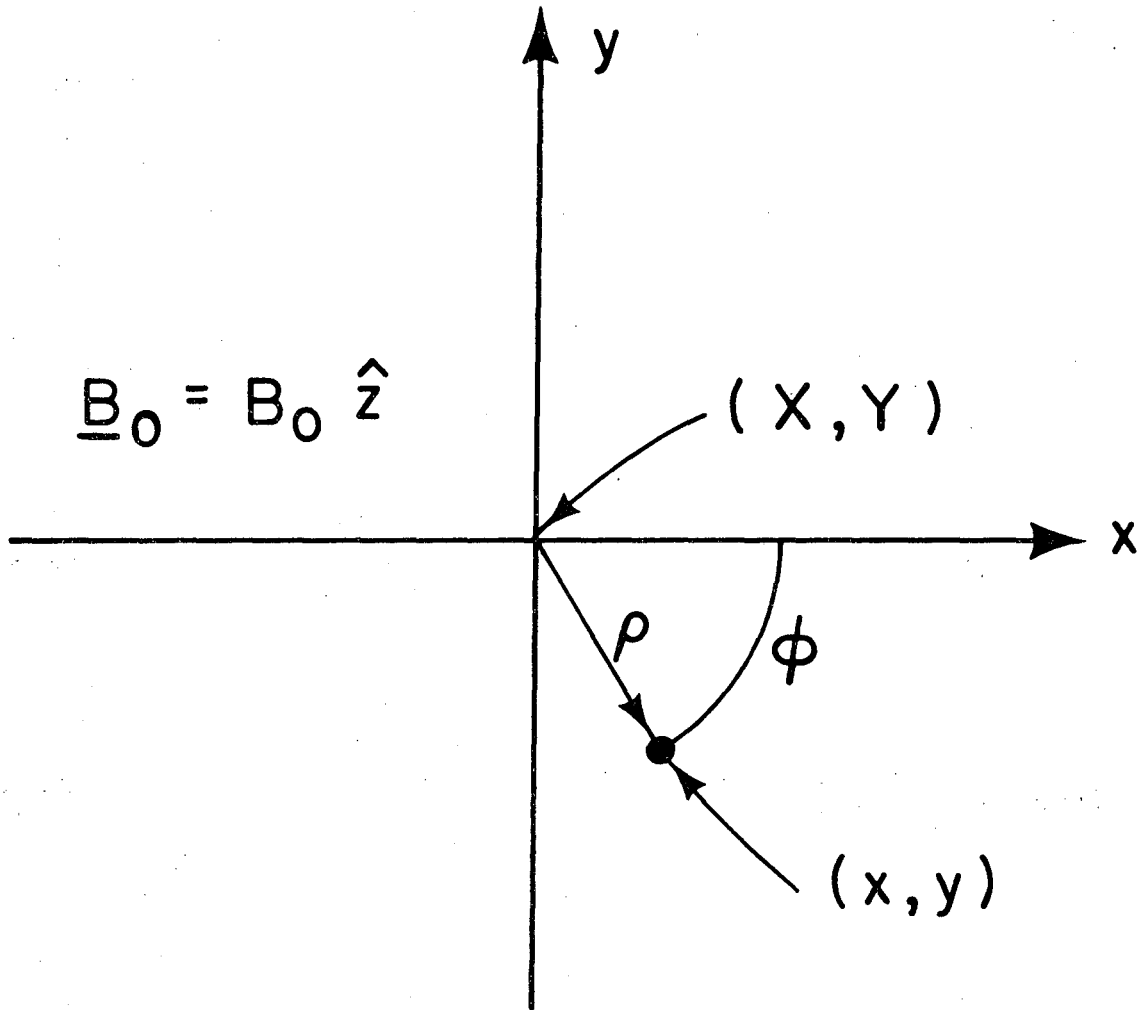
FIG. 6. Particle trajectories, represented by plotting the parallel velocity vs. time. The wave amplitude is given by $\epsilon = 0.75$ and the propagation angle by $\theta = 45^\circ$. The initial speed ($v = 5\Omega/k_z$) and parallel velocity ($v_z = 0$) are the same for all trajectories, but the initial phases $k_z z$ and ϕ differ.

FIG. 7. The mean square deviation in parallel velocity vs. time. Parameters are the same as in Fig. 6.

FIG. 8. Dispersion diagram (ω vs. k) for a plasma in a uniform magnetic field, showing the high-frequency Alfvén wave (Appendix A), the ion-acoustic wave (Secs. XI and XII), and the low-frequency ion-acoustic wave (Sec. XI). Adapted from a figure in Ref. 45.

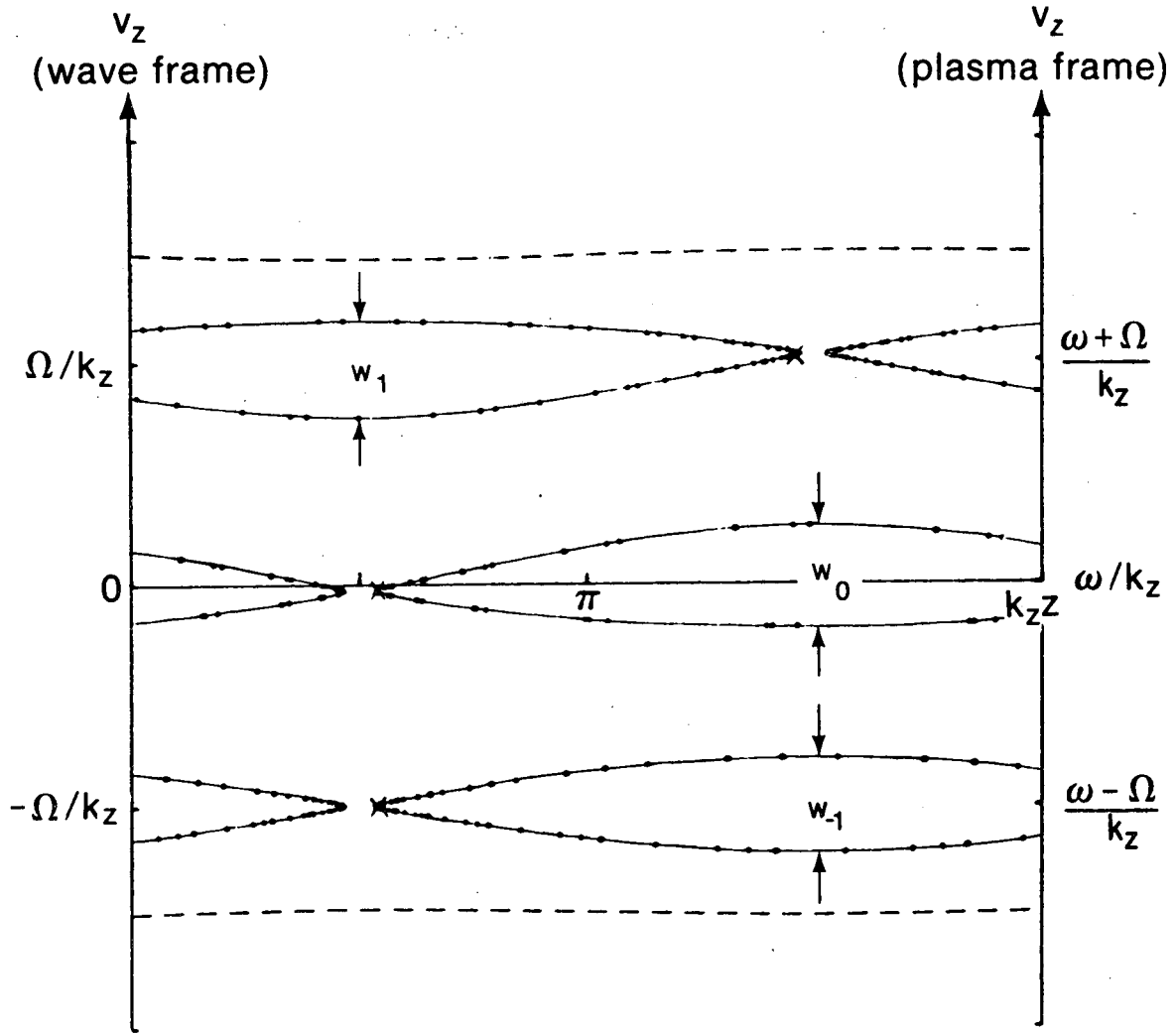
FIG. 9. The perpendicular (f_\perp) and parallel (f_\parallel) distribution functions in the presence of a finite-amplitude, obliquely propagating, electrostatic wave. The distortions to Maxwellian distributions ($\epsilon = 0$) are shown for two wave

amplitudes, $\epsilon = 0.25$ and 0.75 .



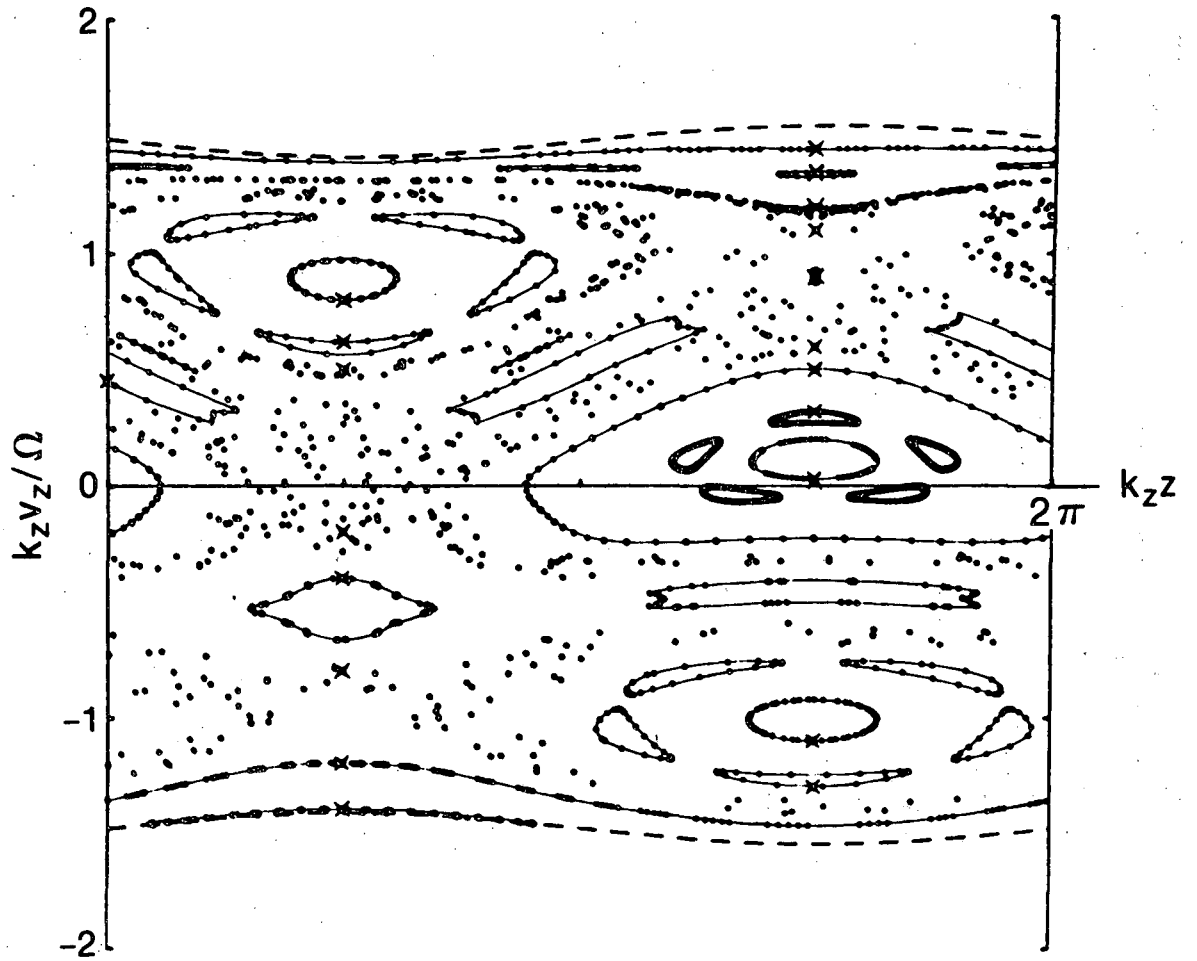
XBL773 - 613

Fig. 1



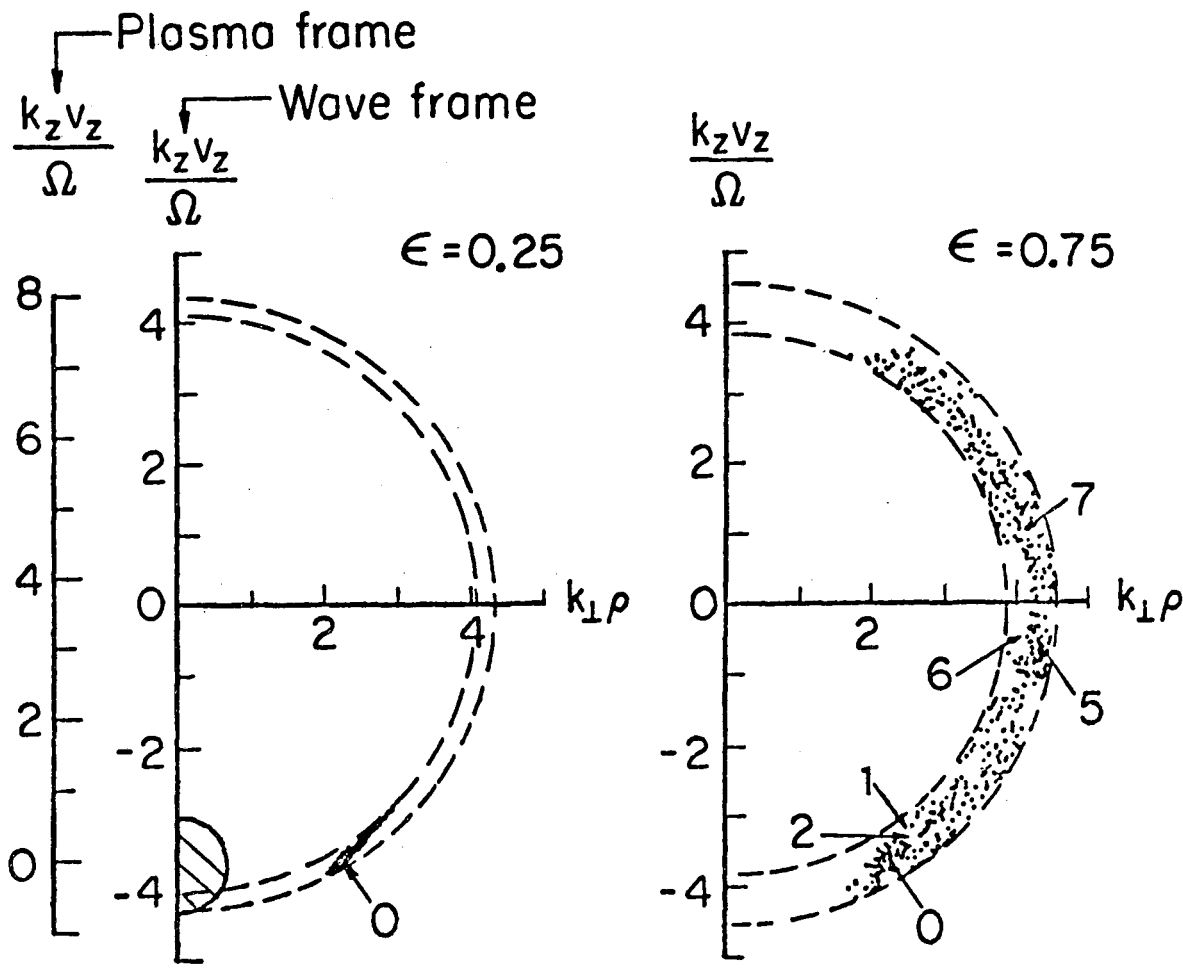
XBL 772-291

Fig. 2



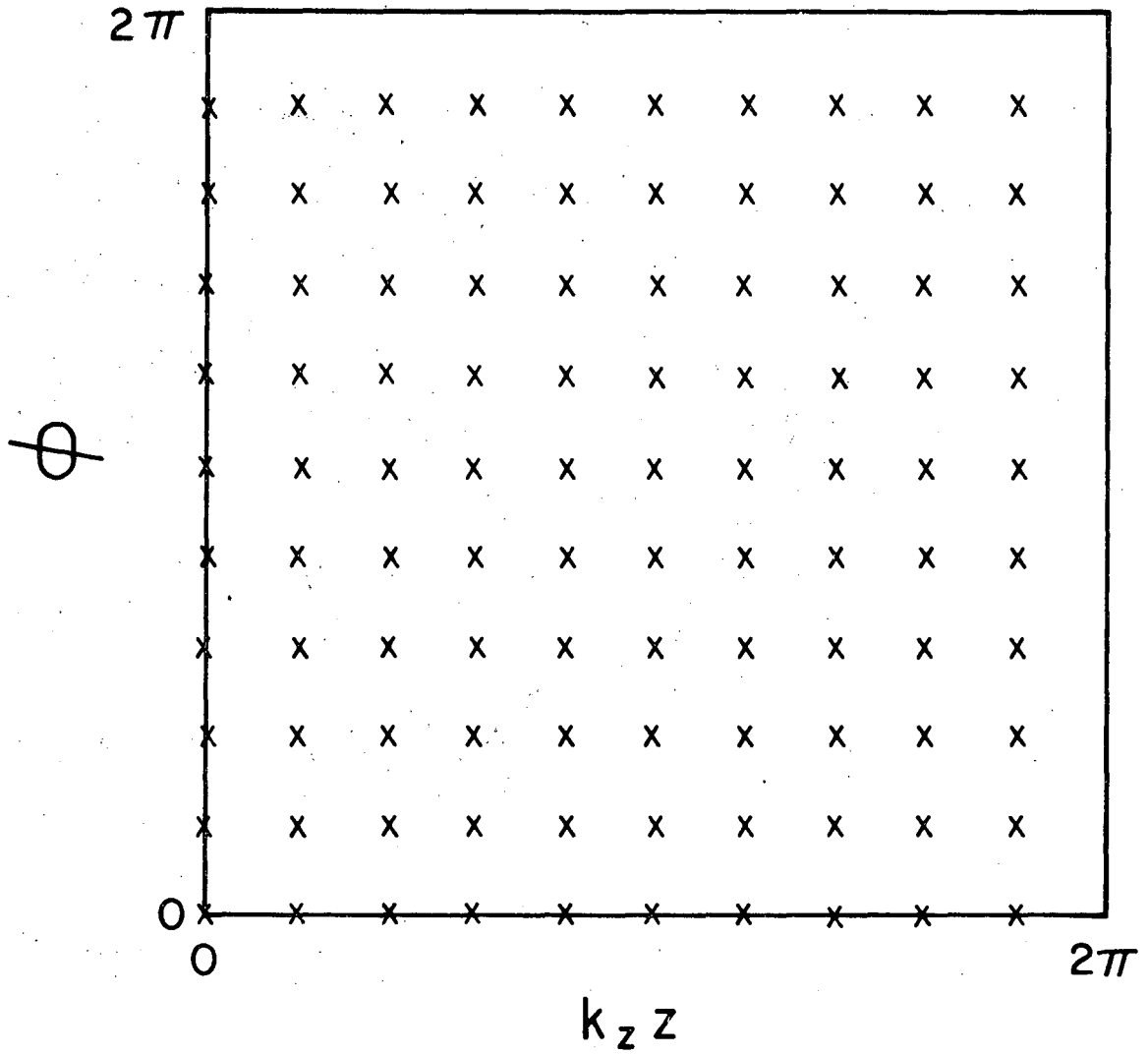
XBL 772-290

Fig. 3



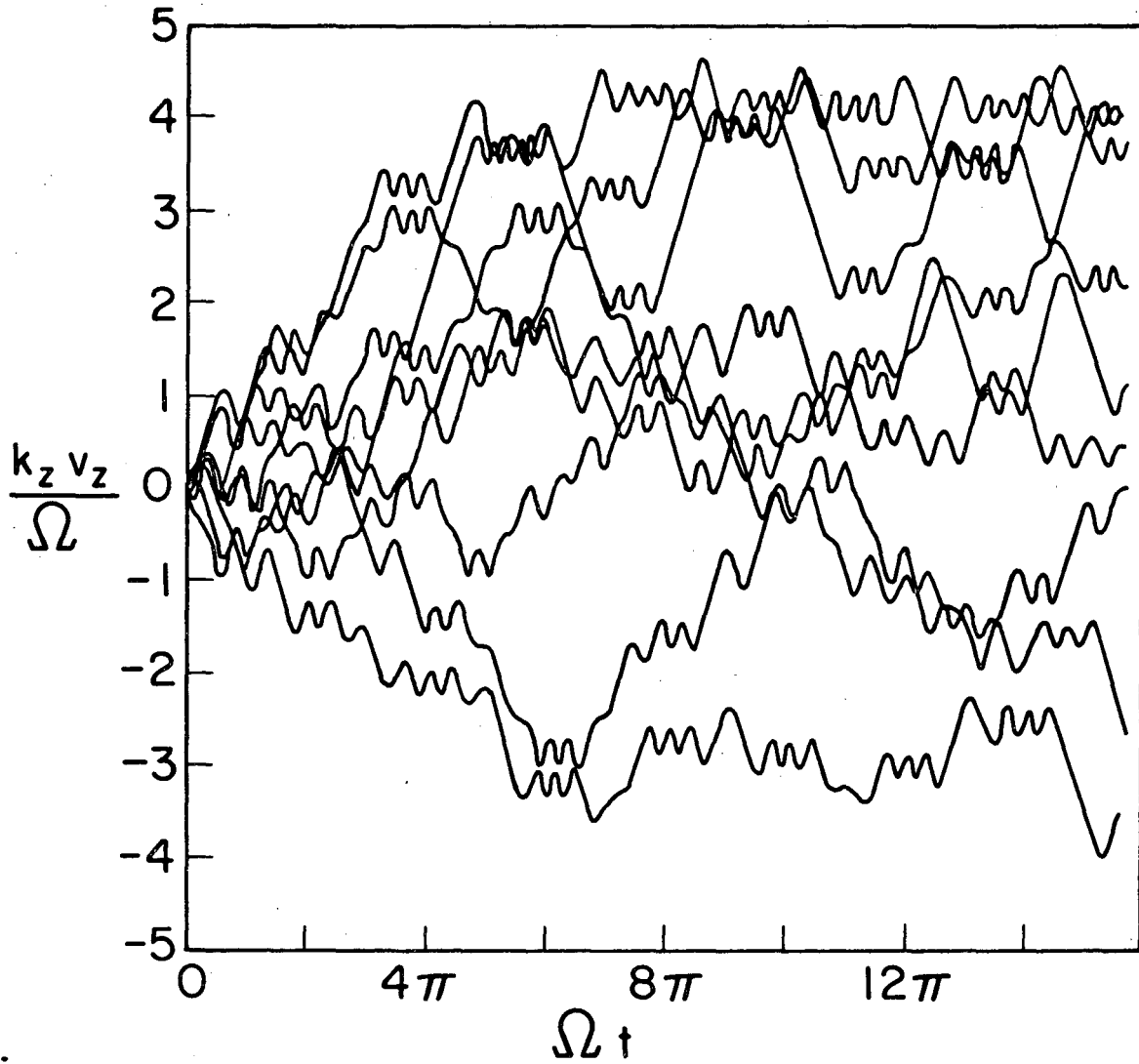
XBL751-2201

Fig. 4



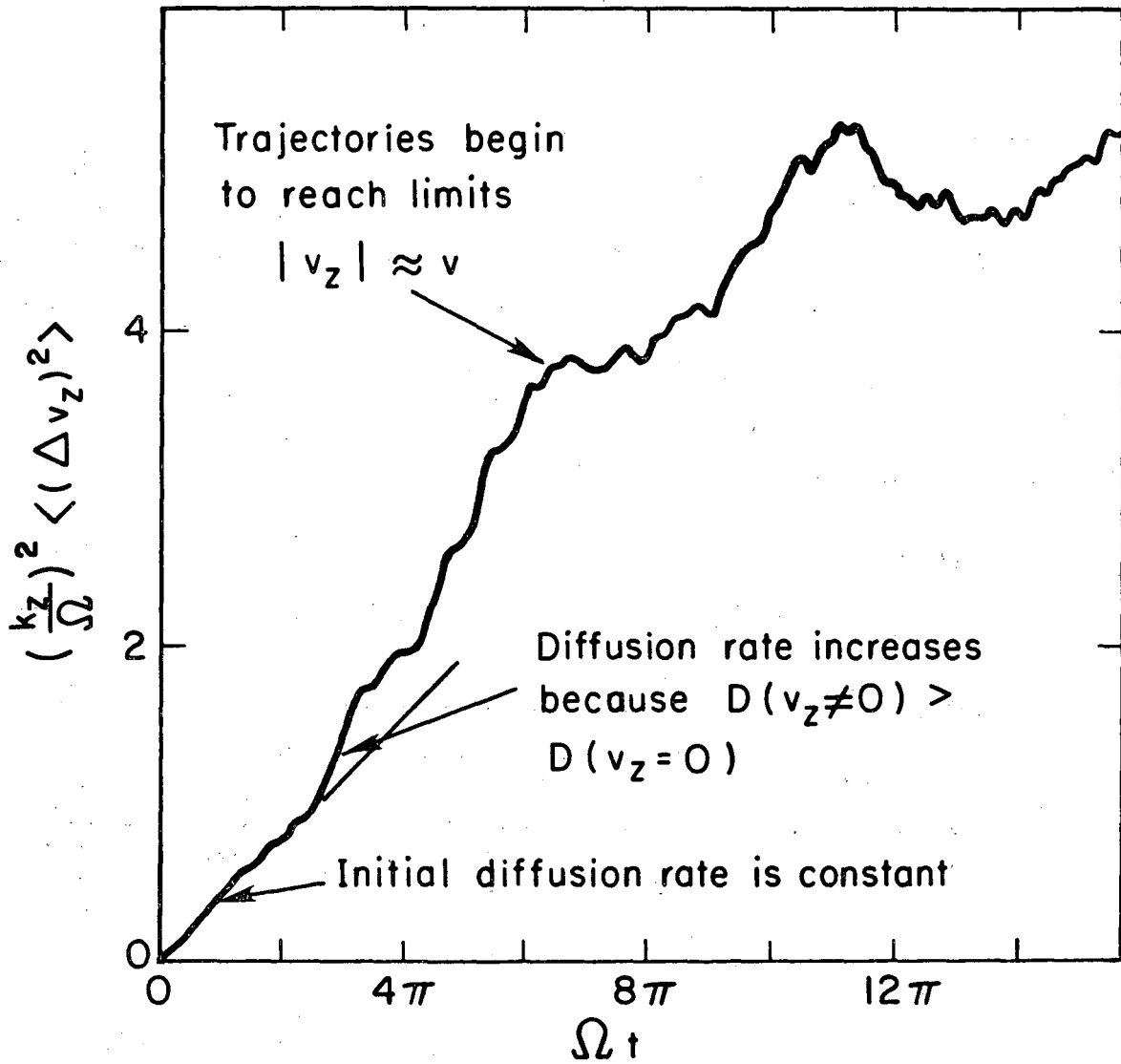
XBL 777-1377

Fig. 5



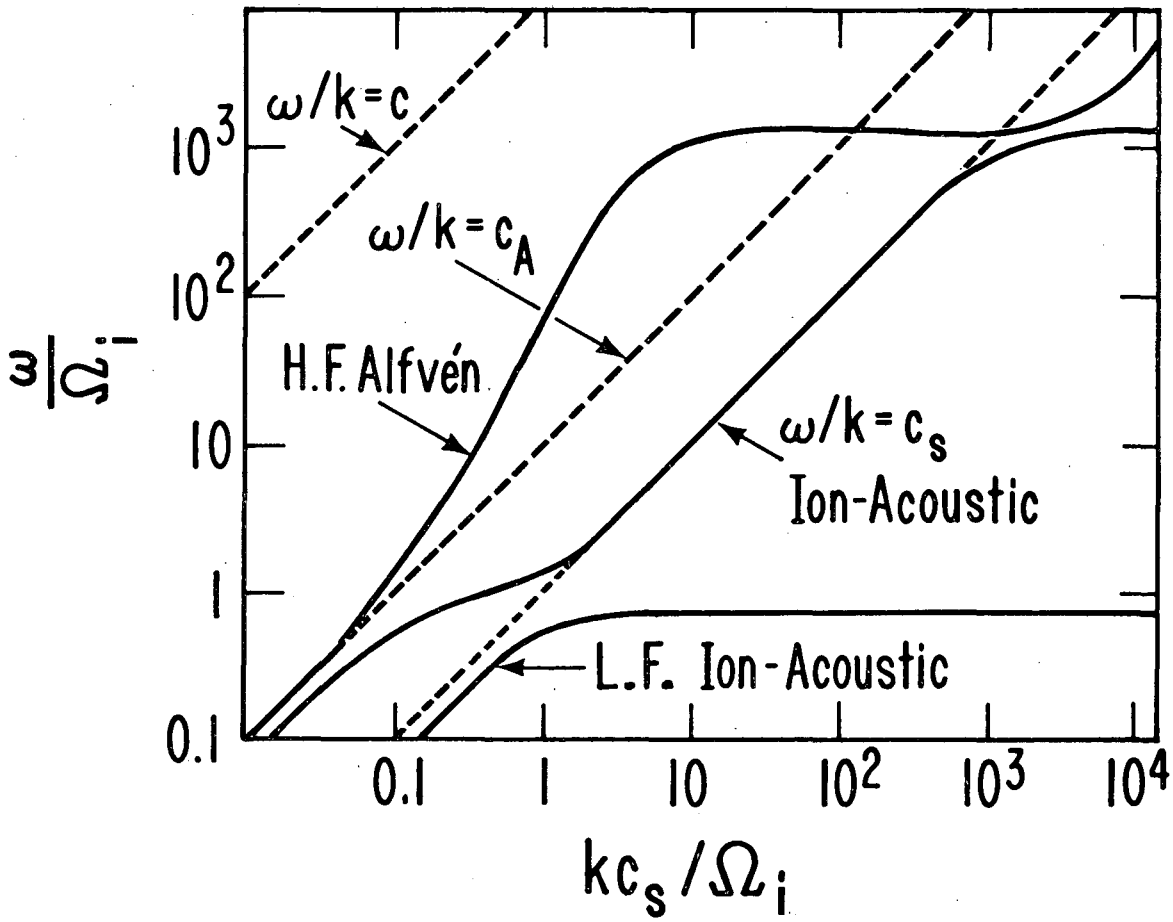
XBL 763-2576

Fig. 6



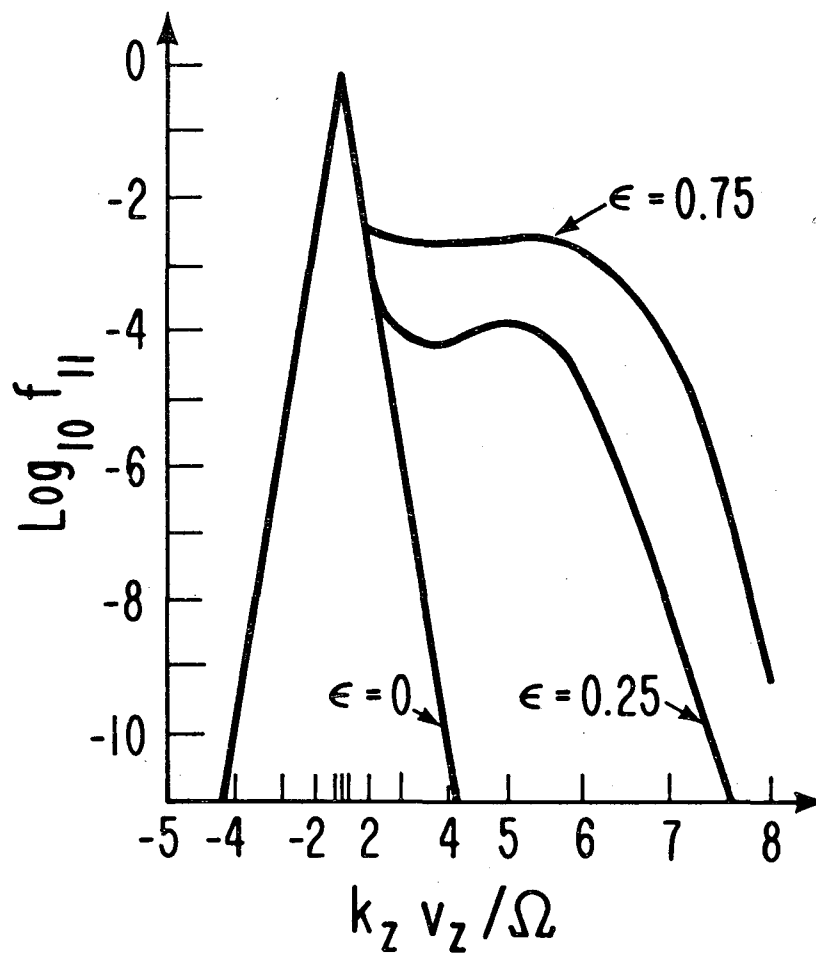
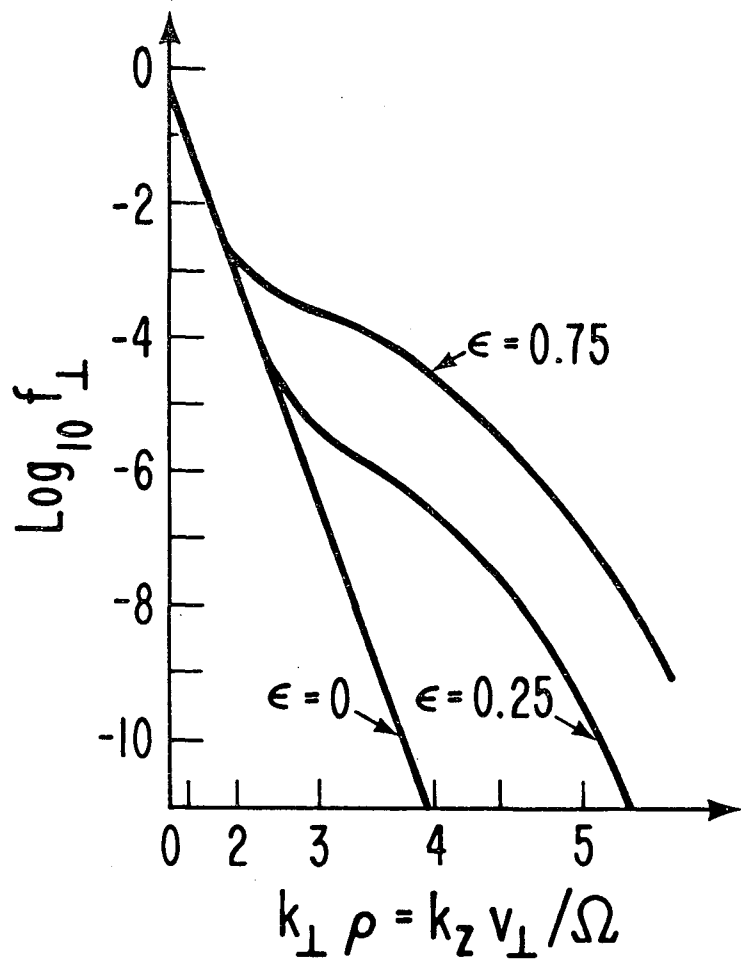
XBL 763-2577

Fig. 7



XBL779-1844

Fig. 8



XBL 779-1845

Fig. 9

This report was done with support from the Department of Energy. Any conclusions or opinions expressed in this report represent solely those of the author(s) and not necessarily those of The Regents of the University of California, the Lawrence Berkeley Laboratory or the Department of Energy.

TECHNICAL INFORMATION DEPARTMENT
LAWRENCE BERKELEY LABORATORY
UNIVERSITY OF CALIFORNIA
BERKELEY, CALIFORNIA 94720